Title
EVALUATION OF THE C-70045A HIGH-SPEED PHOTOMULTIPLIER

Authors
Birk, Meir
Kerns, Quentin A.
Tusting, Robert A.

Publication Date
1964-02-19

UCRL-11147

University of California

Ernest O. Lawrence Radiation Laboratory

EVALUATION OF THE C-70045A HIGH-SPEED PHOTOMULTIPLIER

Berkeley, California

DISCLAIMER

For meeting and Proceedings of
9th Scintillation and Semiconductor
Symposium - Washington D. C.
Feb 26-28, 1964

UCRL-11147

UNIVERSITY OF CALIFORNIA

Lawrence Radiation Laboratory
Berkeley, California

AEC Contract No. W-7405-eng-48

EVALUATION OF THE C-70045A HIGH-SPEED PHOTOMULTIPLIER

Meir Birk, Quentin A. Kerns, and Robert F. Tusting

February 19, 1964

EVALUATION OF THE C-70045A HIGH-SPEED PHOTOMULTIPLIER

Meir Birk,* Quentin A. Kerns, and Robert F. Tusting

Lawrence Radiation Laboratory
University of California
Berkeley, California

I. Introduction

The C-70045A is a high-speed 14-stage photomultiplier developed primarily for scintillation and Cerenkov radiation detection. The tubes were developed by the Radio Corporation of America under contract No. AT(30-1)-3032 to the Division of Biology and Medicine of the U. S. Atomic Energy Commission. [1]

A photograph of the C-70045A is given in Fig. 1. The fully-curved transmission-type photocathode is located on the side of the metal envelope. The electron-lens system is designed to focus electrons from the cathode into the multiplier section with a small time spread. Accelerating electrodes are located between successive dynodes to reduce time spread within the electron-multiplier structure. The anode circuit of the tube has been incorporated into a 50-Ω transmission system with the center conductor of a coaxial connector as the output terminal.

Since the C-70045A was developed for high-speed timing application, measurements were made primarily to determine time spread, pulse response, and other characteristics important to its time-resolving capabilities. Measurements were made using the divider network suggested by RCA. A schematic diagram of the divider and tube is given in Fig. 2. The operating voltage of the tube is the voltage applied between the cathode and the output connector shell and does not include voltage between the anode and the output connector shell. All tubes were degaussed before testing; previous experience has shown this to be a necessary precaution.

II. Photocathode and Electron-Lens System.

The C-70045A photomultiplier has a fully-curved transmission-type side-window cathode with extended S-11 response. The specified minimum useful diameter is 1-1/4 in. and the radius of curvature of the spherical faceplate is 2.56 inches. Average photocathode quantum efficiencies (at 4200 Å) of the eight tubes tested range from 14 to 23% with a mean of 19.5%. Connection to the cathode is made by way of the metal envelope of the tube.

The three-element electron-lens system has circular geometry. Since the entry region to the first dynode is more nearly rectangular than circular, additional electrodes are needed to focus electrons into the multiplier. A cross-sectional view of the electron optical system and the first few dynodes is given in Fig. 3. Focusing electrodes 1 and 3 and the shield are normally operated at dynode 5 potential, and focusing electrode 2 is internally connected to the cathode. Internally connected to the dynode 5 are the two wires marked F_1 and F_2. It was necessary to adjust the deflector voltage for each tube individually in order to optimize collection efficiency. The optimum value of deflector voltage was found to be within approximately 200 V of dynode 5 potential.

With the recommended divider and an operating voltage of 4.5 kV, electrons are first accelerated to 1500 eV as they pass through the lens system and then are decelerated to 900 eV before striking the first dynode. The resulting mean cathode-to-first-dynode transit time at 4.5 kV is 7 nsec. (See Section VII for a discussion of transit time.)

A. Quantum and Collection Efficiency Uniformity.

Curves showing the uniformity of the product of quantum efficiency and collection efficiency across the tube face are given in Fig. 4 for a typical tube (No. 22). The solid line shows the relative pulse amplitude obtained when the tube is scanned with a small light spot in a direction parallel to the long direction of dynode 1, through the center of the photocathode. The dashed curve is the result of scanning in a direction perpendicular to dynode 1. It is seen from the figure that the most efficient region of the photocathode is a roughly rectangular area 1-1/2 by 3/4 in. in size. This area may be considered to be the image of the sensitive region of dynode 1 projected onto the photocathode. The fall-off of the dashed curve is due primarily to reduced collection efficiency rather than a reduced quantum efficiency. A triggered light source was used for this measurement. [2,3] The operating phototube voltage was 4.4 kV, with the voltage distribution given by the RCA divider. The deflector voltage was set for maximum average photoelectron collection over a 1-1/4-in. -diameter circle.

B. Cathode-to-First-Dynode Transit-Time Difference.

Cathode-to-first-dynode transit-time difference was measured by successively illuminating 3/16-in. -diameter areas of the photocathode, with a mercury switch light source, along lines parallel to and perpendicular to the long axis of dynode 1. The time of arrival of the anode pulse was measured (using the leading-edge half-height point of the pulse) with a sampling oscilloscope triggered by an electrical pulse from the light-flash generator. [4] Figure 5 is the transit-time-difference curve for tube No. 22 with an operating voltage of 4.4 kV.

The variation in transit time correlated with position of illumination is seen to be 150 psec or less within 5/8 in. of the center of the photocathode. Other C-70045A tubes have similarly small position-dependent transit-time variations over a 1-1/4-in. -diameter area of the cathode. The magnitude of the measured cathode-to-first-dynode transit-time difference is in good agreement with the predictions of Matheson of RCA.[5] It is interesting to note, however, that the shapes of the cathode transit-time-difference curves obtained from several tubes are not similar, indicating that these position-dependent time variations could be reduced by closer mechanical tolerances in the lens system, but even if these position-dependent effects were entirely eliminated, overall timing accuracy would not be markedly changed.

The cathode-to-first-dynode transit-time difference is a systematic effect. In addition to this effect one must consider variations in cathode-to-first-dynode transit time due to the initial velocity spread of emitted electrons. With an estimated electric field at the cathode of 100 V/cm (operating voltage 4.5 kV) the time variation due to initial velocity is calculated to be about 200 psec.[6,7] The time variation with initial velocity follows a relation of the form

$$\Delta t = \frac{v_0}{E(e/m)}$$

where

v_0 = initial velocity,
E = electric field,
e/m = charge-to-mass ratio.

III. Multiplier Section

The 14-stage multiplier section of the C-70045A uses the central-potential design developed by Dr. George Morton of RCA.[8,9] The central-potential multiplier structure differs from a conventional electron multiplier in that it has an additional set of electrodes located between the dynodes (refer to Figs. 3 and 6). These accelerating electrodes are operated at a high voltage with respect to the adjacent dynodes to produce an acceleration-deceleration effect for each multiplier stage. With the recommended voltage divider network and a tube operating voltage of 4.5 kV, the interdynode voltage is 150 V, while the voltage between the first dynode (D_1) and accelerating electrode 1 (A_1), D_2 and A_2, etc. is 1.5 kV (refer to Fig. 2). This arrangement provides a high electric field at the surface of the dynodes, reducing interdynode transit-time variations due to the spread in secondary emission velocities. The transit time through the multiplier structure, however, is similar to that of conventional 14-stage multipliers since the interdynode spacing has been made larger to provide room for the accelerating electrodes.

IV. Output Structure

In order that the bandwidth of the C-70045A not be limited by the output structure, the anode has been formed into a transmission system of approximately constant impedance. Connection to the anode is made by way of the BNC connector (refer to Figs. 1 and 6). The outer conductor of the BNC is connected within the tube to two tapered metal strips (the anode shields of Fig. 6.) which are the outer conductors of a strip transmission line of 50 Ω characteristic impedance. Accelerating electrodes 15 and 16 and the grid are connected to the ends of the anode shields to make the anode surroundings electrically continuous. The grid screens the anode from approaching electrons until the electrons are about 3 mm from the anode. With a voltage between D_{14} and the anode of 2 kV, the time of flight of electrons between the grid and anode is approximately 100 psec.

Not shown in Fig. 6 are the internal capacitors which bypass the last few dynodes. The drawing is not quite right in showing the grid position: the grid is actually located closer to A_{15} than indicated.

V. Direct Current Gain and Dark Current

The dc gain and anode dark-current characteristics were measured using the recommended voltage divider (see Fig. 2). In addition, the anode of the tube was biased 300 V positive with respect to the output connector shell to ensure that electrons leaving D_{14} would be collected primarily by the anode rather than by the electrodes which form a shield surrounding the anode. The potential of the deflector was adjusted for maximum dc gain. Figure 7 is the curve of dc gain and anode dark current of tube No. 1-7-64 as a function of the voltage applied between the photocathode and the output connector shell. (One notes in Fig. 7 that the anode dark current is nearly constant at the low tube voltage. The 35 pA of anode current at zero applied voltage is due to ohmic leakage from the anode of the tube.) Several of the photomultipliers tested had similar gain and dark-current characteristics, although others had larger dark current. Few further measurements were made on tubes of high dark current since we felt that they were not representative of production tubes of this type.

Both the gain and dark-current characteristics are dependent on whether the tube is operated with the anode biased positive with respect to its surroundings (see Fig. 6). With positive bias, the dc gain and anode dark current of these tubes are typically 10 to 100 times higher and the pulse gain approximately 5 times higher than with zero bias. The effect of the bias on the pulse shape is marked, and will be discussed more fully later in this report. We did not specifically measure the bias-related gain shift and fatigue effects which might exist in the C-70045A at various counting rates but we believe that the effect of anode bias should be considered if one wished to use the tube in an application where stability of gain is important.[10]

VI. Pulse Tests of the C-70045A

Pulse tests were made using the voltage

divider network suggested by RCA. The deflector potential was adjusted to obtain the best average collection efficiency over the central 1-1/4 in. of the photocathode. (The deflector potential when adjusted this way is not significantly different from that which gives maximum dc gain.) A minor misadjustment of the voltage on the deflector has the expected effect of shifting the peak collection efficiency area of the cathode perpendicular to the axis of D_1, (refer to the dashed curve of Fig. 4).

Tests were made to determine the effects of anode bias on the output pulse shape, amplitude, and the current-saturation characteristics. A mercury switch light-pulse generator[4] was used for many of the measurements. We also used a Cerenkov radiator light source for time measurements.

A. Impulse Response

The impulse response of the C-70045A was measured using a 1 Gc/sec oscilloscope and light flashes from cosmic ray Cerenkov radiation. (We used a Tektronix type 519 traveling-wave oscilloscope with a vertical sensitivity of 10 V/cm and sweep speeds to 2 nsec/cm.) The Cerenkov radiator was a 1-in.-long lucite rod (index of refraction ≈ 1.5) 1 in. in diameter, in direct optical contact with the photocathode, and liberated approximately 25 photoelectrons. Typical output pulses are shown in the oscillogram of Fig. 8; the time scale is 4 nsec per division. The lower trace was obtained with the anode biased +300 V with respect to the output connector shell and the upper trace with zero volts bias. As can be seen, the rise time of the tube is approximately 0.5 nsec. Output pulses produced by single-electrons from the photocathode have a similar shape (except for a slightly faster rise time), indicating that the fall time ($\tau \approx 3$ nsec) of the pulse does not depend upon the number of photoelectrons leaving the photocathode. The fall time therefore is related to effects within the multiplier and the output section of the tube.

B. The Effect of Anode Bias upon a Train of Light Flashes

The response of the C-70045A to a burst of pulses was investigated by illuminating the cathode with a train of flashes from four corona lamps separated in time by 5 nsec.[2,3] The peak light intensity from each lamp was adjusted to a common value. Oscillograms of the output pulse burst are given in Fig. 9 for the cases of 0 and +300 V anode bias. The vertical scale is 100 mV per major division. Operating voltage of the tube is 4600 V, and the light level is the same for both oscillograms.

C. Current Saturation

The pulse current saturation characteristics of C-70045A No. 1-7-64 operated at 4.8 kV are given in Fig. 10. With the anode biased +300 V with respect to the output connector the saturation current is 250 mA, about 2-1/2 times greater than with zero bias.

When the tube is operated within its linear range, the output current pulse due to a short light flash (≈ 1 nsec or less) is about half the amplitude and half the width with zero bias as with positive anode bias. For progressively longer pulses, the main effect of positive anode bias is to increase the gain about a factor of 5 without changing the pulse shape.

From a gain-bandwidth point of view, it appears reasonable to state that varying the anode bias has the effect of changing the gain without changing the gain-bandwidth product. Additional work needs to be done to clarify the observed effects.

VII. Transit Time

The total transit time as a function of operating voltage is given in Table I for tube No. 6, and was measured from the half-height point on the leading edge of the light flash reaching the photocathode to the half-height point of the leading edge of the anode pulse arriving at the BNC connector.

Table I. Total transit time as a function of opating voltage.

Operating Voltage, V (kV)	Total Transit Time, T (nsec)
3.00	40.33
3.50	37.12
4.00	34.79
4.50	32.71
5.00	31.03
5.50	29.49
6.00	28.11

The electrons move within the phototube at sufficiently low velocity that relativistic effects are small and the speed v of the electrons can be expressed as $v = \sqrt{2Ve/m}$, where V is the appropriate fraction of the operating voltage. One then expects transit time to obey a relation of the form

$$T \sqrt{\frac{k}{V}} + T_0$$

The numbers in Table I do fit such a relation, with a standard deviation of about 50 psec. The transit time of the electron cascade from dynode 1 to the output connector was measured by directly illuminating dynode 1 with a focused spot of light from the light flasher. The time so obtained is multiplier transit time. By subtracting the multiplier transit time from the total transit time, one finds the cathode-to-first-dynode transit time to be 7 nsec at 4.5 kV operating voltage.

The dimensions of the photomultiplier tube

are such that there is a flight path of the electron cascade as it moves from cathode to D_1, D_1 to D_2, etc., which totals about 21 inches. There is an additional 3 in. of electromagnetic signal flight path on the transmission line between the anode and the BNC output connector. At 4.5 kV operating voltage, where the interdynode voltage is 150 V per stage, the mean electron velocity in the multiplier is 0.058 c (where c is the velocity of light), which corresponds to the velocity of an 860-eV electron. Without the central potential electrodes, the mean velocity would have been that of a 37.5-eV electron; on the other hand, a closer dynode spacing would then be appropriate.

In the photocathode and electron-lens system, the mean velocity of electrons is 0.045 c when the tube operates at 4.5 kV.

Slight dimensional differences from one phototube to another will cause individual differences in total transit time, but the trend of Table I appears in all C-70045A photomultipliers.

VIII. Transit-Time Spread

Single-electron transit-time spread of the C-70045A was measured in the following way: The photocathode was exposed to flashes from a high-speed light source that has such low intensity that most of the flashes produce no photoelectrons.[11] Then the probability of a given light flash producing r photoelectron is given by the Poisson equation: $P_r = \epsilon^r e^{-\epsilon}/r!$, where ϵ is the expected number of photoelectrons per light flash. For sufficiently small ϵ, $P_1 \approx \epsilon$, and the probability of more than a single electron per flash is very small. The time of emission of the electrons from the photocathode (neglecting time delay in photoemission) has a probability distribution that has the same shape as the curve of intensity as a function of time for the light flash[11,12]

The difference is measured between the time of arrival of a photomultiplier anode pulse (resulting from a single photoelectron) and time of occurrence of the light flash. A large number of such measurements is made and the results are plotted as a histogram of the number of anode pulses having a particular delay with respect to the light flash. The shape of the histogram approaches the convolution of the functions representing the transit-time spread of the photomultiplier and the form of the light flash.

It is found in the present measurements that the C-70045A photomultiplier and the mercury switch light source have time distributions of similar durations but different shapes. A practical problem in making measurements is that photomultiplier pulses resulting from single electrons have a wide range of amplitudes. We have chosen to include pulses within an amplitude range of 25:1, to minimize the possibility of an error from a correlation between amplitude and timing.

The measurement of the time between the light flash and a phototube anode pulse can be performed in a variety of ways. We chose the relatively simple method of photographing traces on an oscilloscope and measuring the pictures with a micrometer-stage-equipped microscope. The oscilloscope sweep is triggered by the light-flash generator. A small marker pulse from the light source is introduced on the trace several nanoseconds in advance of the expected photomultiplier pulse. The oscilloscope sweeps once for each light flash. Most traces contain only the marker pulse since the expected number of photoelectrons per flash is much less than one, but a few traces have both the marker and a phototube pulse. Figure 11 is an oscillogram of typical traces used for the measurement. The traces without pulses are used to calculate ϵ and predict the contamination of the data by multiple-electron pulses.

We estimate P_0, the probability of obtaining no output pulse for a given light flash:

$$P_0 = 1 - \frac{\text{Number of traces with a pulse}}{\text{Total number of traces}} = e^{-\epsilon} \approx 0.80.$$

It follows that: $\epsilon \approx 0.224$,
$P_1 \approx 0.18$,
$P_{r>1} \approx 0.02$.

In this case, the percent of pulses that are due to more than a single electron leaving the cathode per light flash is:

$$100 \times \frac{P_{r>1}}{1 - P_0} \approx 100 \times \frac{0.02}{0.2} \approx 10\%.$$

A 10% contamination of the data by multiple-electron pulses has a relatively minor effect on the time-spread distribution.

Figure 12 shows a histogram of the time distribution of pulses from tube No. 6 operated at 6.0 kV and measured in the above way. The anode of the tube is operated at +300 V with respect to the output connector, and only the center 1-in. diameter of the photocathode is illuminated. Time of the phototube pulse was measured by using the leading-edge half-height point. The full width at half maximum (fwhm) of the distribution is approximately 360 psec. As mentioned earlier, the observed time distribution of the output pulses depends on both the light-flash shape and the time spread of the tube.

The technique described by Koechlin was used to unfold the distribution of Fig. 12.[13] With the assumption (which gives a reasonably good fit to the data) that the light flash from the mercury switch light source has an exponential decay, we calculate the fwhm of the photomultiplier single-electron time distribution to be 320 psec. From our calculations, the light-flash decay time constant is approximately 300 psec, and its rise time is short compared to 300 psec.

It is appropriate here to point out that the width of the light flash from the mercury switch pulse generator depends strongly upon its operating voltage. To achieve the short pulses we describe here, it is necessary to keep the voltage below 200 V. (The wave shape described in the literature has been measured at approximately

1000 V.)[4]

IX. Scintillator Measurements

The fast response of the C-70045A photomultiplier enabled us to measure the scintillation decay time of plastic scintillators. The scintillators tested were Lawrence Radiation Laboratory plastic scintillator (polystyrene ≈ 97.5%, p-terphenyl 2.5%, tetraphenylbutadiene 0.03% and zinc tetrate 0.01%) and "Naton 136" (Nash and Thompson, Ltd., Hook Rise, Tolworth, Surrey, England.) Both scintillators were machined to fit the cathode surface of the tube and had the shape of a cylinder 1 in. in diameter and 1 in. long. Also an identical Cerenkov radiator was prepared to serve as a prompt source of light. The three cylinders were placed in turn on tube No. 6, and the anode current pulses caused by cosmic rays were recorded on a Tektronix 519 oscilloscope (rise time ≈ 0.3 nsec). In each of the three cases, several pulses were photographed, normalized to the same height, and a mean pulse shape was drawn.

An anode current pulse caused by a scintillator is the convolution of the scintillation function over the response function of the system to a delta function of light. This system function was obtained by using the Cerenkov radiator. We were thus able to try various scintillation functions and see whether the results of their convolutions over the known system function fitted the anode pulse shapes obtained experimentally.

Using a digital computer to numerically evaluate the required convolutions, it was found that in the two scintillators tested, the assumption of a pure exponential decay gave a reasonably good fit. The decay-time constants were found to be 3.8 nsec for the LRL plastic scintillator and 2.1 nsec for "Naton 136". The estimated accuracy of these figures is ±15%.

A comparison of the light efficiencies of the two scintillators was made, using gamma rays from Cs^{137} and from Na^{22}. The comparison was made by integrating the first 10 nsec of the anode current pulse. It was concluded that the efficiences of the two scintillators were equal to within 10% in total number of photoelectrons emitted. One may therefore conclude that "Naton 136" has a considerable advantage over the LRL scintillator for timing purposes.

X. Summary and Conclusions

Some of the more important timing parameters of the tube are summarized below.

A. Rise Time

One should consider two cases for rise time:

1. Impulse response (δ-function light input), and
2. Step response (step-function light input).

1. Impulse Response. We have approximated a light impulse in two different ways: (a) by registering single-photoelectron events, and (b) by employing a 1-in.-diameter Cerenkov radiator to excite the photocathode. The output current pulses due to Cerenkov input (see Fig. 8) are not appreciably broader than those due to single-electron events. Under conditions of zero anode bias and 4.8 kV operating voltage, the output pulse has a fwhm of 0.84 nsec after correction for the cable and oscillograph system. The pulse shape is roughly Gaussian, although on close inspection it appears blunted somewhat like a cosine-squared pulse. The 10 to 90% rise time is 450 psec; this is the result for a Cerenkov light-flash input.

2. Step Response. The rise time to a step function of light is longer than the rise to an impulse. If the tube behaved as a linear system, one would anticipate the step-response to be the time integral of the impulse-response, leading to a value of approximately 1.45 nsec for the 10 to 90% rise time. Photographs of the output current pulse due to the plastic scintillator excited by electrons show a mean rise time of 1.53 nsec at 4.8 kV operating voltage. The scintillator rise time of 0.65 nsec imposes a small correction; within the experimental error of the measurement one can say that the step-function rise time of the tube is approximately 1.5 nsec, 10 to 90%.

B. Time Jitter

The single-photoelectron time distribution of the tube at 6 kV operating voltage has been measured. It is approximately Gaussian in form, with a fwhm of 320 psec. (The rms deviation from the mean = σ = 320/2.355 = 136 psec.) A correction for oscilloscope bandwidth is not required in this measurement. It is useful to consider separately the various sources of time jitter and their magnitudes in the present tube:

Quantity	Cause	Magnitude
1. Multiplier time spread τ_1	Geometrical imperfections and finite initial velocity of secondary electrons.	257 psec, fwhm
2. Photocathode-to-D_1 time spread τ_2	Depends on initial emission velocity spread of photoelectrons and is therefore sensitive to color of illumination.	175 psec, fwhm
3. Photocathode transit-time difference τ_3	Geometrical—depends on path-length differences and electric-field nonuniformity primarily at the photocathode	80 psec, fwhm

It is not possible to find precise time distributions for the various causes of jitter without great effort. For simplicity, we assume Gaussian errors and add them in rms fashion:

Overall time jitter = $\sqrt{\tau_1^2 + \tau_2^2 + \tau_3^2}$ = 320 psec, fwhm.

It is clear that if $\tau_3 \to 0$ the overall time jitter would not change appreciably, thus τ_3 is not a limitation at present. One should remember that the 320-psec value refers to the single-electron time spread. If a light flash evokes N coincident electrons, the tube time spread shrinks by $\sqrt{N}$ and other effects may dominate in determining system time spread. We found, for a pair of C-70045A photomultipliers viewing a Cerenkov radiator in coincidence, a time spread which could be almost entirely accounted for by optical-path-length differences related to the position of arriving particles. (As a matter of interest, a plane optical wavefront arriving at the curved photocathode strikes the center first and the edges approximately 30 psec later.)

The capability of the C-70045A in resolving closely spaced pulses appears superior to that of any other phototube of equal gain. Evidently Cerenkov pulses as close as 2 nsec can be counted separately if one uses the proper circuits. To take full advantage of these capabilities requires high gain. It is to be hoped that with further production of this tube type, the gain can be increased and dark current improved.

Acknowledgments

This work was done under the auspices of the U. S. Atomic Energy Commission. We would like to thank Philip Dunn for his assistance in making some of the measurements.

Figure Captions

Fig. 1. The C-70045A photomultiplier.

Fig. 2. Schematic diagram of the C-70045A and voltage divider network.

Fig. 3. Cathode-to-first-dynode electron-lens system and first few multiplier stages of the C-70045A.

Fig. 4. Curves showing the product of quantum efficiency and collection efficiency across the photocathode of C-70045A No. 22. The solid curve is the result of scanning along a line parallel to the long axis of the first dynode. The dashed curve is the result of scanning perpendicular to the first dynode.

Fig. 5. Cathode transit-time-difference curves for C-70045A No. 22. The solid curve was obtained by successively illuminating 3/16-in.-diameter areas of the photocathode along a line parallel to the long axis of the first dynode. The dashed curve is the result of a measurement in the perpendicular direction.

Fig. 6. Output structure and last few multiplier stages of the C-70045A.

Fig. 7. Gain and dark-current characteristics of tube No. 1-7-64 with the voltage distribution provided by the divider network of Fig. 2. The anode was biased +300 V with respect to the output connector.

Fig. 8. Output pulses from tube No. 1-7-64 operated at 4.8 kV due to impulse light flashes from a Cerenkov radiator. The lower trace was obtained with +300-V anode bias and the upper waveform with zero anode bias. The time scale is 4 nsec per division.

Fig. 9. Output current waveform from the C-70045A resulting from a burst of four light flashes separated in time by 5 nsec. The vertical scale is 2 mA per major division and the time scale is 5 nsec per major division. The lower waveform was obtained with +300-V anode bias and the upper with zero bias.

Fig. 10. Pulse current-saturation characteristics of tube No. 1-7-64 operated at 4.8 kV.

Fig. 11. Single-photoelectron pulses from C-70045A No. 6 operated at 6 kV. The small positive pulses are the time reference marks used in the measurement of single-electron time spread. The precursor or "front-porch" noted here has been eliminated in production tubes (compare with Fig. 8).

Fig. 12. Transit-time-difference histogram for single-photoelectron pulses from tube No. 6 operated at 6.0 kV.

Footnote and References

*Present address: Weizmann Institute of Science Rehovoth, Israel.

1. R. M. Matheson, "Recent Photomultiplier Developments at RCA," Ninth Scintillation and Semiconductor Counter Symposium, Feb. 26-28, 1964, Washington, D. C.

2. T. G. Innes and Q. A. Kerns, "A Pulsed Nanosecond Light Source," Lawrence Radiation Laboratory Report UCRL-9726, Aug. 4, 1961 (unpublished).

3. Q. A. Kerns and G. C. Cox, "A Triggered Nanosecond Light Source," Nucl. Instr. Methods 12, 32 (1961).

4. Q. A. Kerns, F. A. Kirsten, and G. C. Cox, "Generator of Nanosecond Light Pulses for Phototube Testing," Rev. Sci. Instr. 30, 31 (1959).

5. "Proposal for Development of a Photomultiplier Having a Pulse Rise Time Less Than 5×10^{-10} Second (C70, 045)," Electron Tube Division of Radio Corporation of America, November 17, 1961.

6. G. Pietri, "Progress in Photomultiplier Tubes for Scintillation Counting and Nuclear Physics," IRE Trans. Nucl. Sci. NS-9, No. 3, June 1962, p. 62.

7. G. Pietri, "Photomultipliers in Experimental Physics — Problems Encountered in Design, Production, and Use," Acta Electronica 5, 7 (1961).

8. George A. Morton, R. W. Matheson, and M. H. Greenblatt, "Design of Photomultipliers for the Sub-Millimicrosecond Region," IRE Trans. Nucl. Sci. NS-5, Dec. 1958.

9. George A. Morton, "High-Speed Photomultipliers and Electronic Devices," in Proceedings of the 2nd Symposium on Advances in Fast-Pulse Techniques for Nuclear Counting, Berkeley, California, February 1959 (Lawrence Radiation Laboratory Report UCRL-8706, 1959), pp. 13-19.

10. R. B. Murray, "Scintillation Counters," in Nuclear Instruments and Their Uses, Arthur H. Snell, ed. (John Wiley & Sons, Inc., New York, 1962), Chap. 2, pp. 135-36.

11. R. F. Tusting, Q. A. Kerns, and H. K. Knudsen, "Photomultiplier Single-Electron Statistics," IRE Trans. Nucl. Sci. NS-9, No. 3, June 1962.

12. L. M. Bollinger and G. E. Thomas, "Measurement of the Time Dependence of Scintillation Intensity by a Delayed-Coincidence Method," Rev. Sci. Instr. 32, 1044 (1961).

13. Yves Koechlin, "Determination of the Form of Very Short Luminous Pulses. Application to Scintillation Phenomena (1962)," Rapport C. E. A. n° 2194, Centre D' Etudes Nucleaires de Saclay, France.

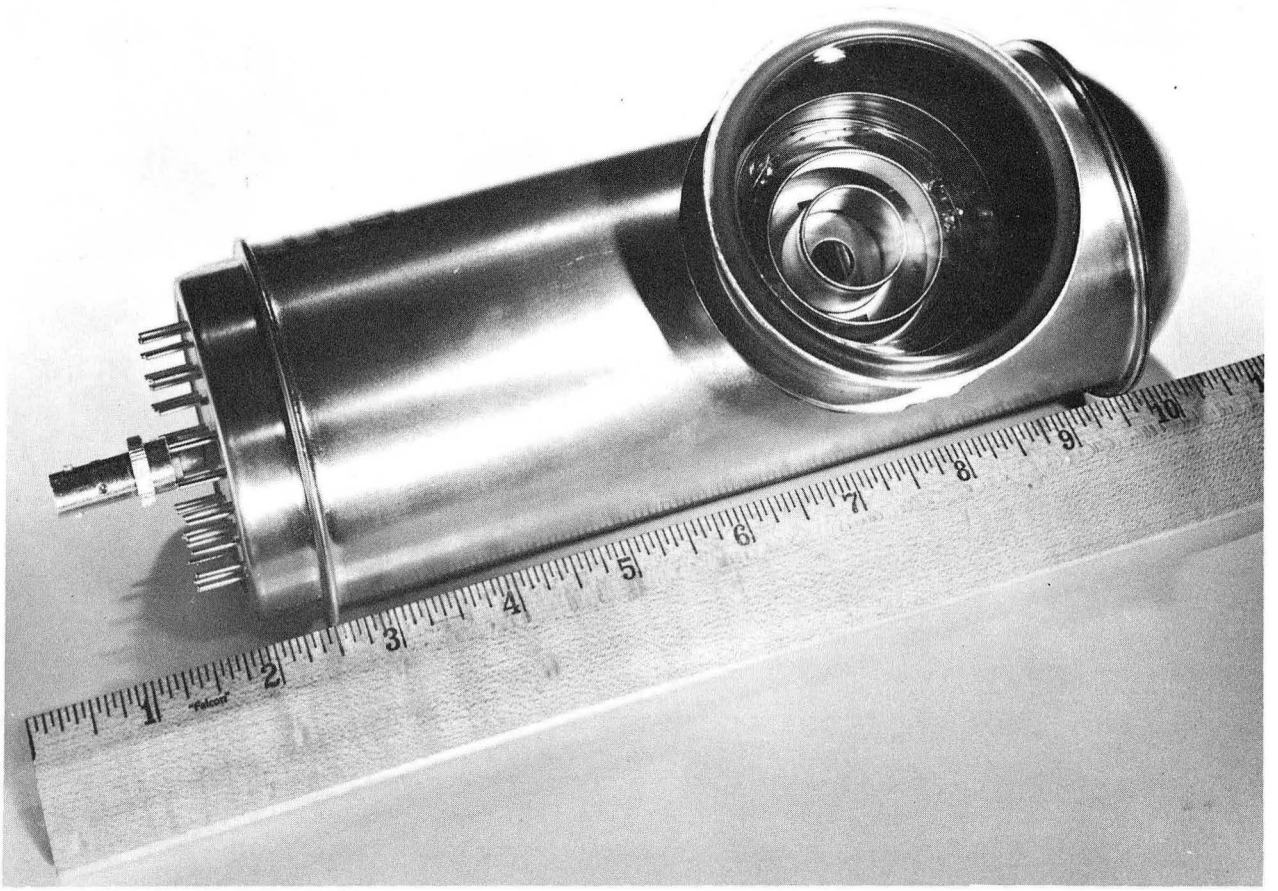

ZN-4138

Fig. 1

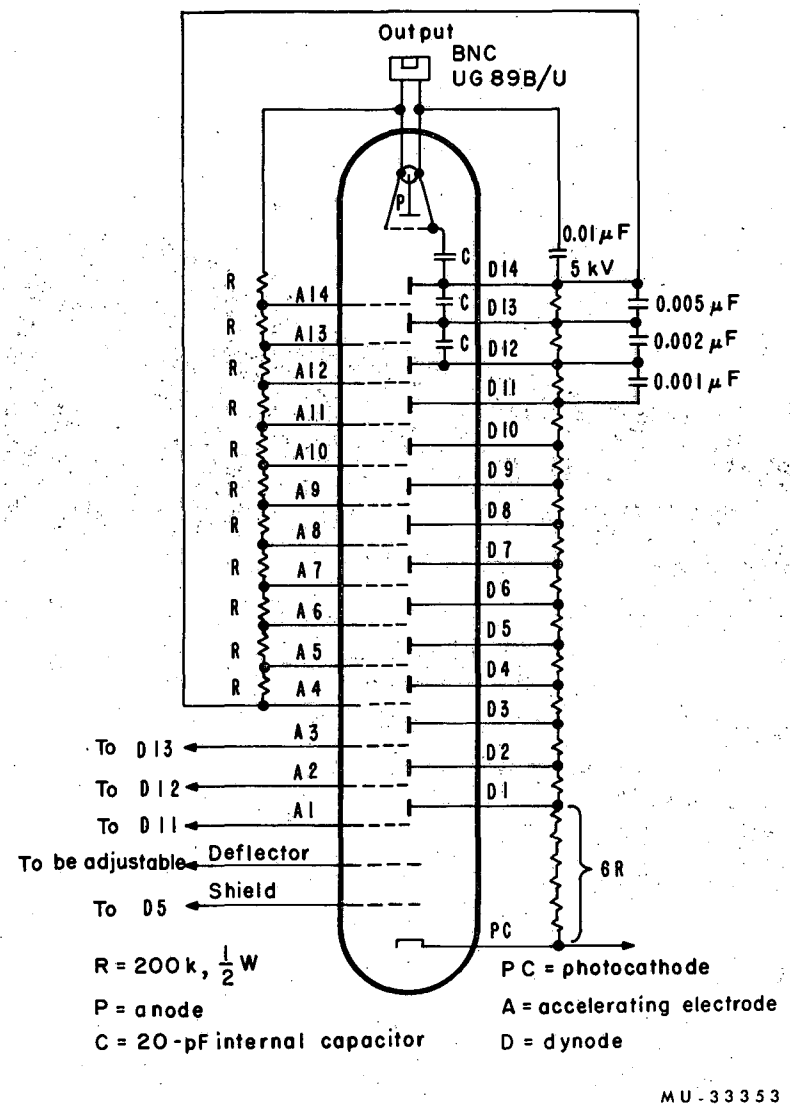
Output
BNC
UG 89B/U
P
C
0.01 μF
5 kV
D14
D13
D12
D11
D10
D9
D8
D7
D6
D5
D4
D3
D2
D1
0.005 μF
0.002 μF
0.001 μF
R
A14
A13
A12
A11
A10
A9
A8
A7
A6
A5
A4
A3
A2
A1
To D13
To D12
To D11
To be adjustable
Deflector
Shield
To D5
6R
PC
R = 200 k, 1/2 W
P = anode
C = 20-pF internal capacitor
P C = photocathode
A = accelerating electrode
D = dynode
MU-33353

Fig. 2

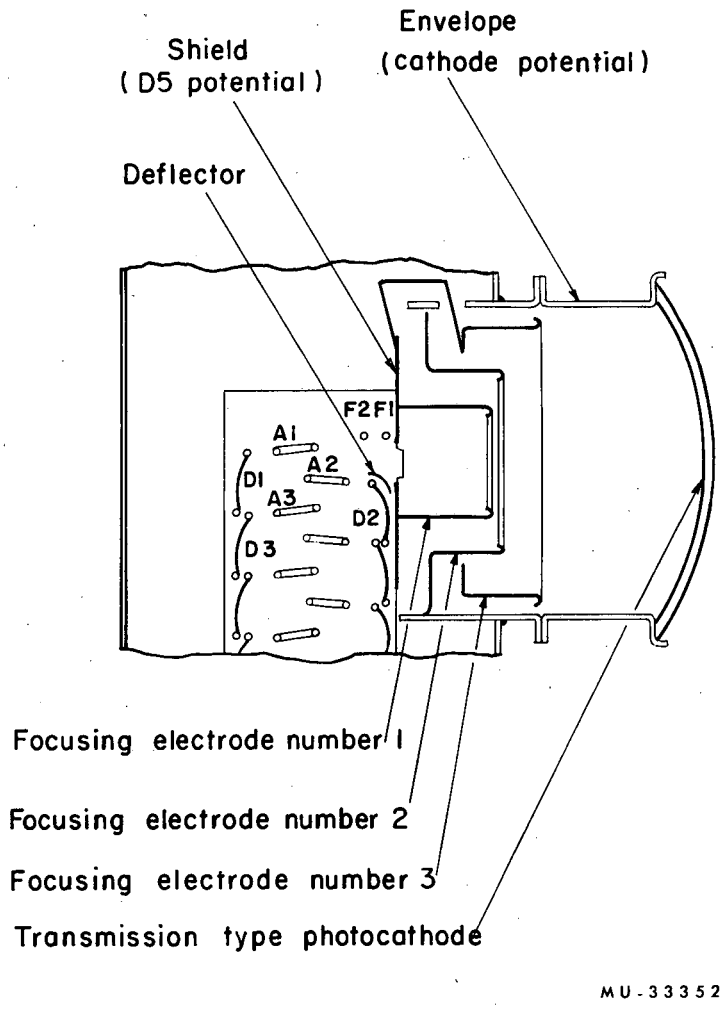
Shield
(D5 potential)
Envelope
(cathode potential)
Deflector
F2F1
A1
A2
D1
A3
D2
D3
Focusing electrode number 1
Focusing electrode number 2
Focusing electrode number 3
Transmission type photocathode
MU-33352

Fig. 3

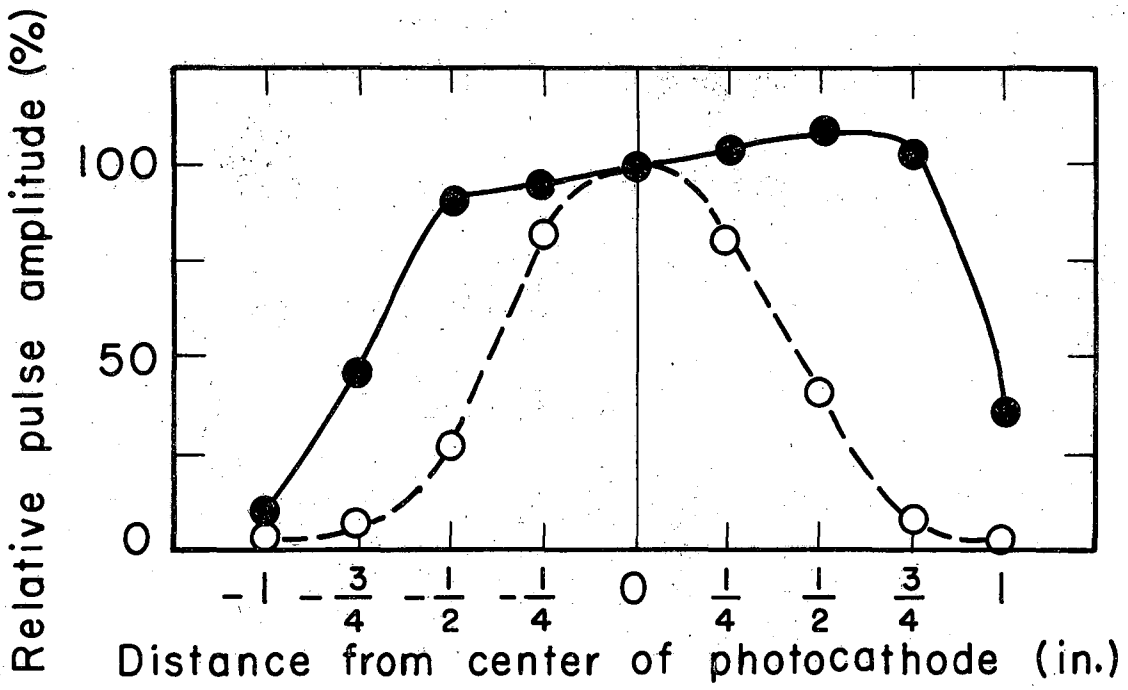
Relative pulse amplitude (%)
100
50
0
-1
-3/4
-1/2
-1/4
0
1/4
1/2
3/4
1
Distance from center of photocathode (in.)
MU-33348

Fig. 4

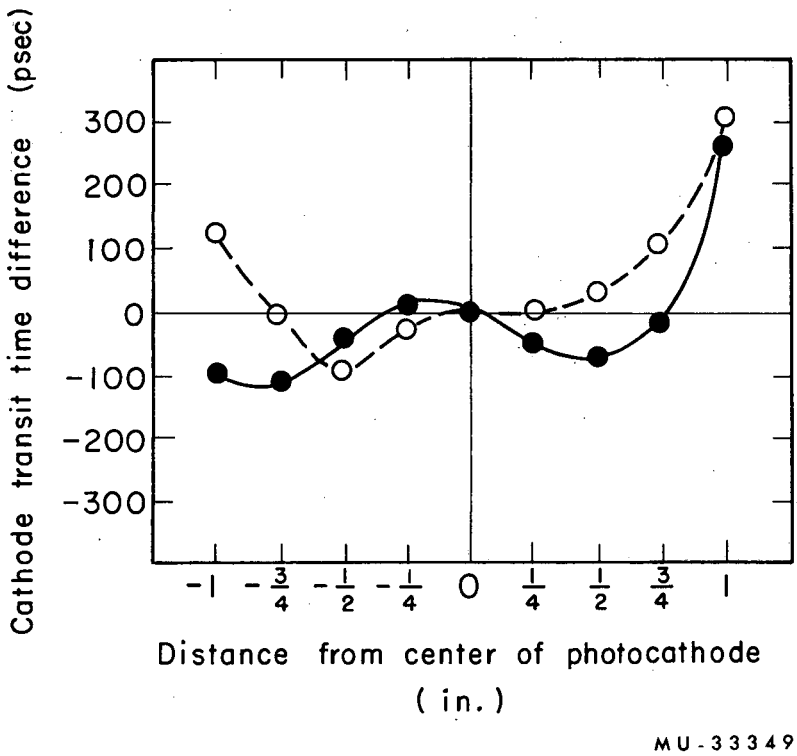
Cathode transit time difference (psec)
300
200
100
0
-100
-200
-300
-1
-3/4
-1/2
-1/4
0
1/4
1/2
3/4
1
Distance from center of photocathode
(in.)
MU-33349

Fig. 5

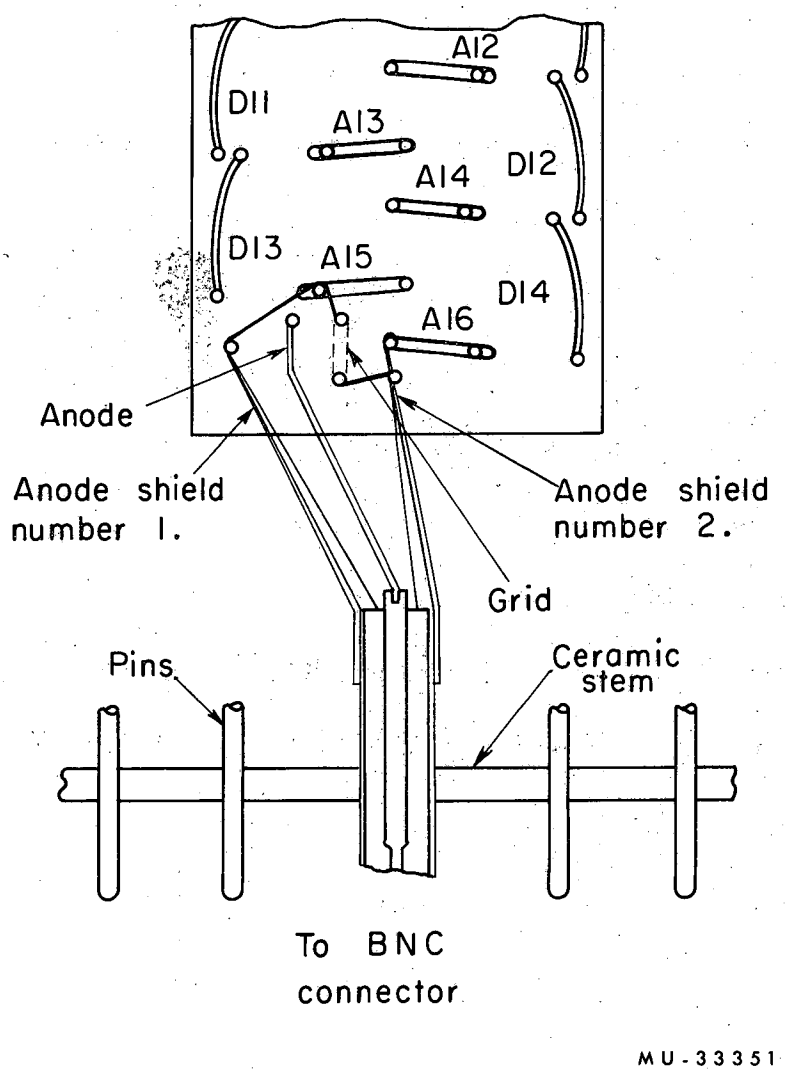
A12
D11
A13
A14
D12
D13
A15
D14
A16
Anode
Anode shield number 1.
Anode shield number 2.
Grid
Pins
Ceramic stem
To BNC connector
MU-33351

Fig. 6

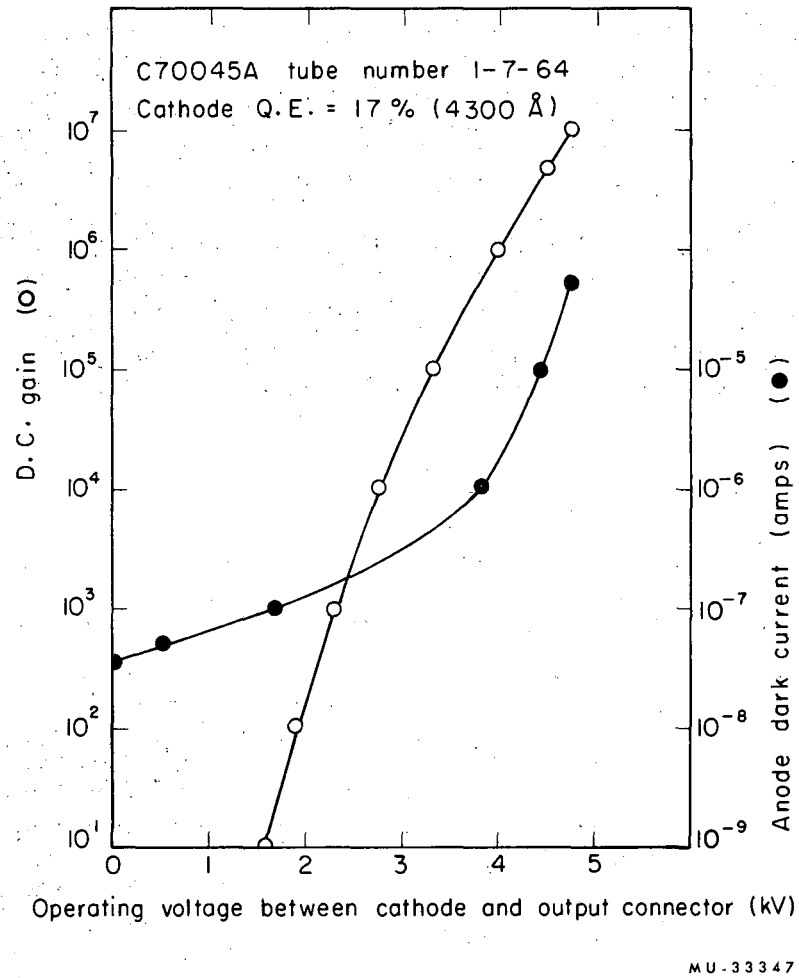
C70045A tube number 1-7-64
Cathode Q.E. = 17 % (4300 Å)
D.C. gain (O)
Anode dark current (amps) (●)
Operating voltage between cathode and output connector (kV)
MU-33347

Fig. 7

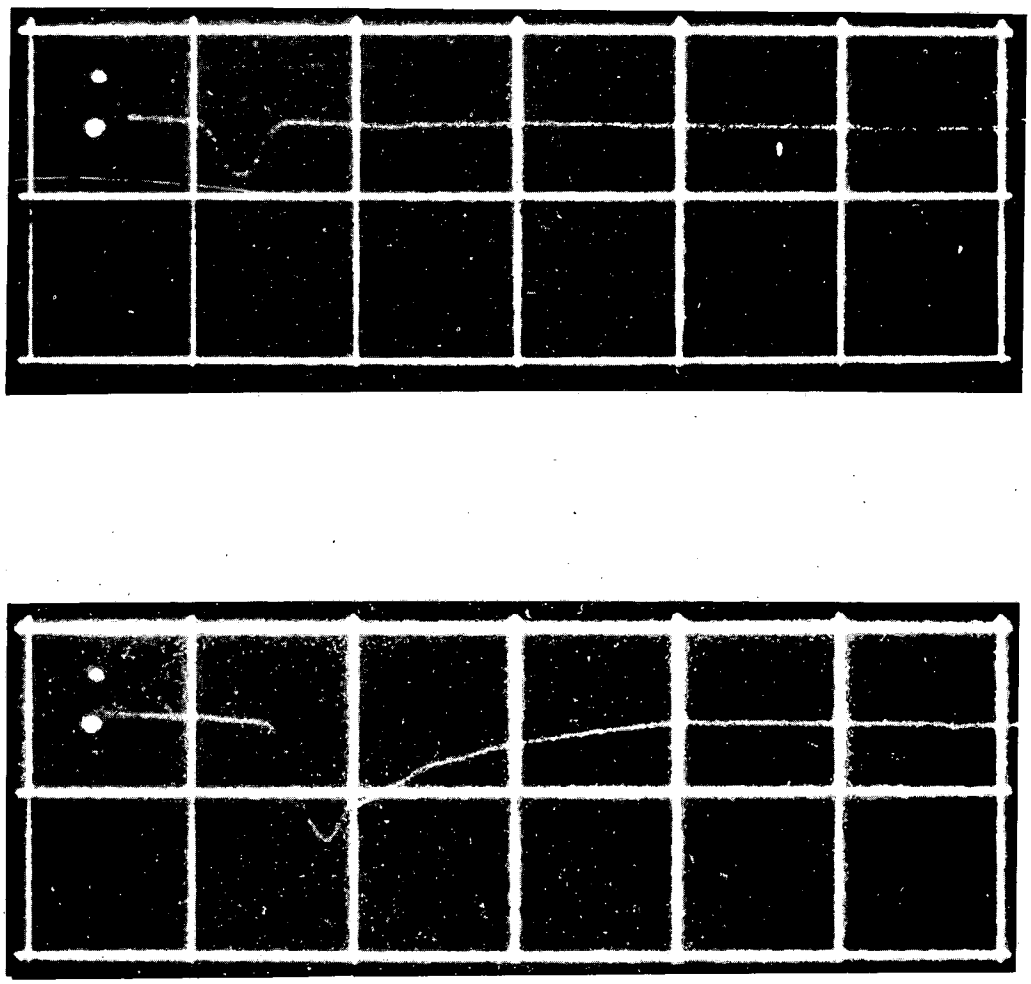

ZN-4141

Fig. 8

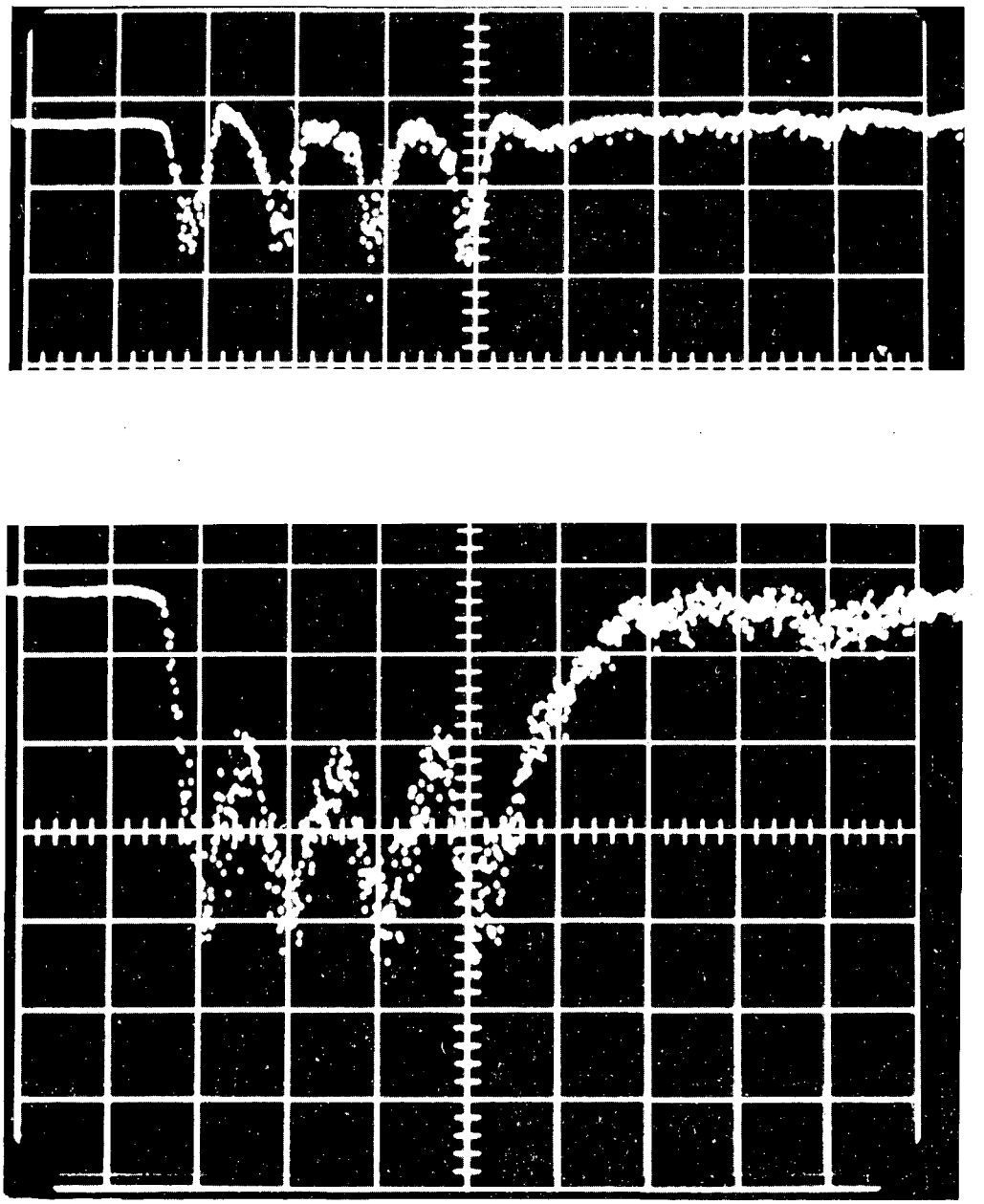

ZN-4140

Fig. 9

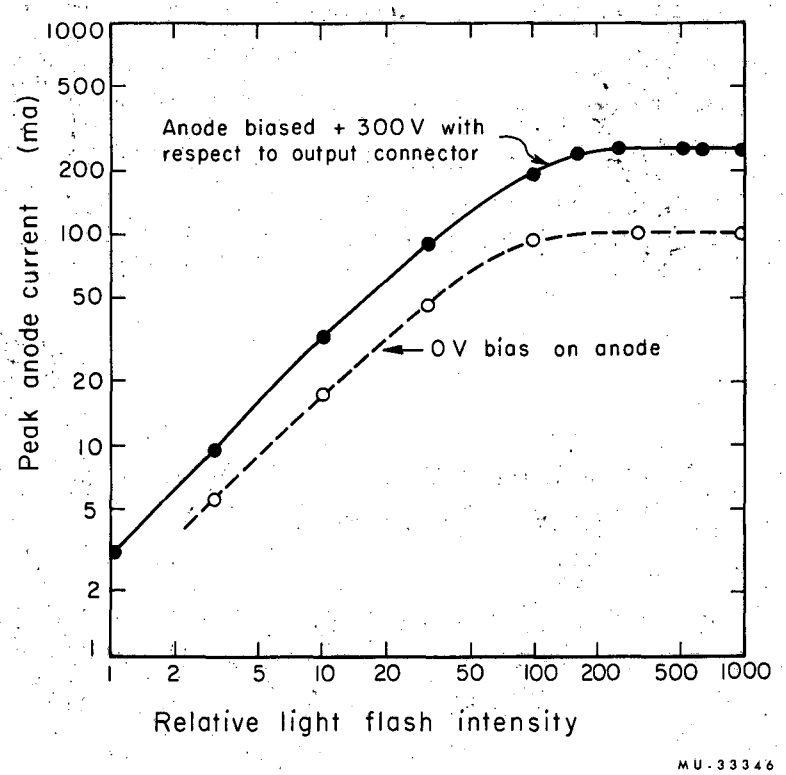
Peak anode current (ma)
1000
500
200
100
50
20
10
5
2
1
Anode biased + 300 V with respect to output connector
0 V bias on anode
1
2
5
10
20
50
100
200
500
1000
Relative light flash intensity
MU-33346

Fig. 10

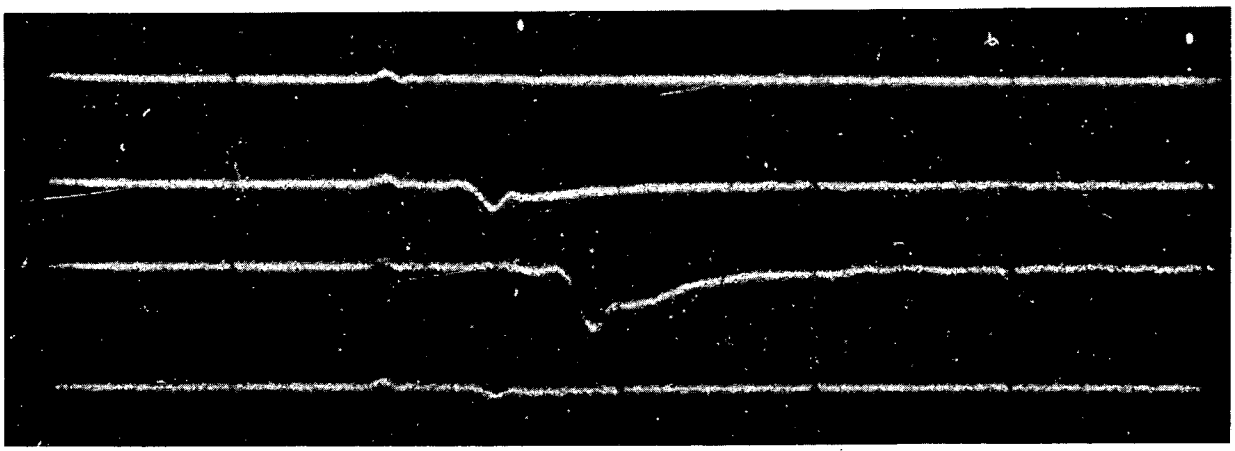

ZN-4139

Fig. 11

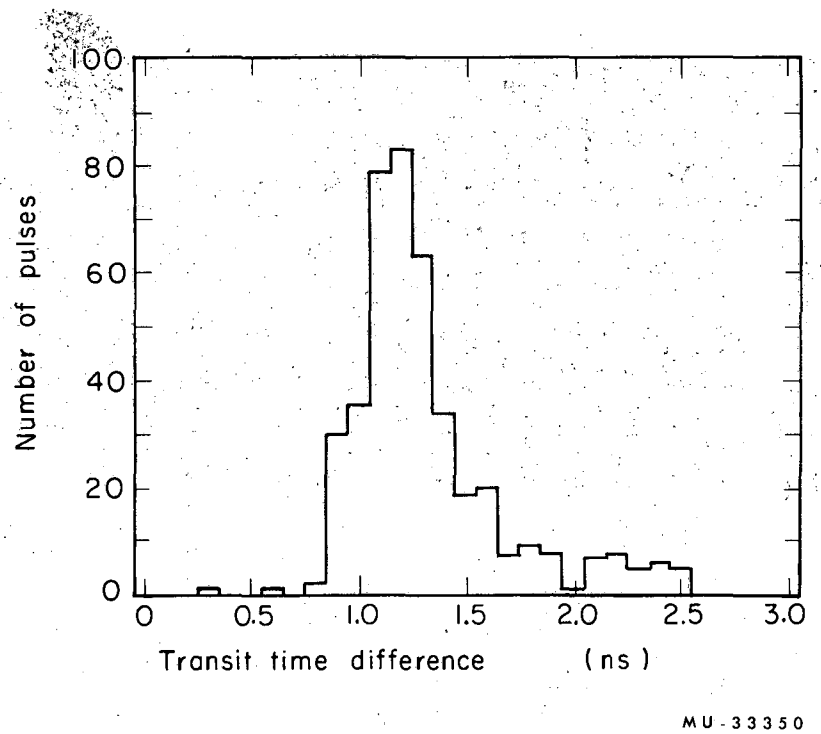
100
80
60
40
20
0
Number of pulses
0
0.5
1.0
1.5
2.0
2.5
3.0
Transit time difference (ns)
MU-33350

Fig. 12